Ionic Liquid-dependent Gold Nanoparticles of Purpurin-18 for Cellular Imaging and Photodynamic Therapy *In Vitro*

Yang Liu, Sang Hyeob Lee, Woo Kyoung Lee,* and Il Yoon*

*Center for Nano Manufacturing and Department of Nanoscience and Engineering, Inje University, Gyeongnam 50834, Republic of Korea. *E-mail: wlee@inje.ac.kr; yoonil71@inje.ac.kr*
Received October 19, 2019, Accepted December 3, 2019, Published online December 20, 2019

Keywords: Ionic liquid, Gold nanoparticle, Photosensitizer, Cellular imaging, Photodynamic therapy

Ionic liquids (ILs) have attracted much attention as promising materials applied in synthesis, catalysis, sensors, electrochemistry, and green and medicinal chemistries based on their interesting properties.[1–4] Besides, ILs can support water solubility and stability of various drugs and promote controlled drug release.[5] Generally, ILs are water-soluble which produces an enhanced hydrophilic environment affecting therapeutic activity.[6,7] Photodynamic therapy (PDT) is patient-specific and noninvasive cancer treatment using the combined therapeutic activity of a photosensitizer (PS), light, and oxygen.[8–11]

To obtain enhanced PDT effect, enough PSs should accumulate in tumor cells, for which a suitable delivery system is important. Gold nanoparticles (GNPs) are promising drug delivery vehicles for highly efficient PDT, photothermal therapy, drug delivery, and biological imaging.[12–15] In addition, GNPs display better penetration into tumor cells and intracellular localization to destroy the cancer cells by inducing apoptosis and necrosis.[16,17] Furthermore, tens of nanometer sized GNPs can preferentially accumulate in tumors by "enhanced permeability and retention (EPR)" effect as a passive targeting.[18]

Recently, we developed a water-soluble IL-type PSs using *N*-methyl-*D*-glucamine to generate GNPs which showed three times higher PDT efficiency than the free PS, indicating that GNPs afforded excellent cellular uptake of the PS and enhanced targeting into tumors due to effective delivery of the GNPs.[19,20]

In this study, we demonstrate IL-dependent PDT of GNPs using two water-soluble IL-type PSs to develop promising PSs with a suitable delivery system for PDT. The synthesis of IL-type PSs (PS1 and PS2) and GNPs (GNP1 and GNP2) was straightforward (Figures S1–S7, Supporting Information). Purpurin-18 (Pu18) was synthesized from methyl pheophorbide a (MPa) in a basic alcohol/ether solvent after acidic extraction from chlorophyll-a paste (Scheme 1).[21] The water-soluble PSs were obtained by treating Pu18 and the ILs morpholinium[5] (PS1) and imidazolium[1,4] (PS2), with hydroxide counter anion (Figure 1 and Scheme S1). Finally, GNPs were prepared by the seed growth method[19,20,22] with some modifications. The GNPs were prepared by reduction method of chloroauric acid ($HAuCl_4$) using the PSs, without any reducing agent and surfactant. The hydroxyethyl unit on each PS has important roles for reduction of the gold ion as well as stabilization of the GNPs (Scheme 2).[19,20,22]

Furthermore, the formation of GNP is stabilized by a strong coordinate-covalent bond between carboxylate of each PS and Au surface.[23]

UV–Vis spectra of PSs and GNPs in aqueous solution (10 μg/mL) are shown in Figure 2(a). The PSs and the GNPs show long-wavelength absorption of the longest wavelength (λ_{max}) at 754–762 nm in water, in which each GNP displays higher absorption intensity as well as longer λ_{max} (red-shift of 7 nm) absorption compared to the corresponding free PS (Table S1). Interestingly, GNP1 displayed higher absorption intensity compared to GNP2 even though the absorption intensities of PS1 and PS2 at λ_{max} were almost the same. Transmission electron microscope (TEM) images of the GNPs are shown in Figure 2(b). TEM images showed that the GNPs had sizes ranging from 20–60 nm and were almost spherical, indicating that the GNPs were well dispersed without aggregation. In addition, thermogravimetric (TGA) analysis (Figure 2(c)) of GNP1 and GNP2 showed 37 and 42 wt % of organic content (PS) and 63 and 58 wt % of inorganic content (Au), respectively. The wt % of organic and inorganic contents in each GNP were used to calculate exact amount of each PS on corresponding GNP (GNP1 contains 492 nmol/mg PS1; GNP2 contains 573 nmol/mg PS2), and used in further cell study.[24]

The dark toxicity and photocytotoxicity of PS1 and PS2, and GNP1 and GNP2 in A549 (human lung adenocarcinoma) cells were evaluated by MTT (3-(4,5-dimethylthiazol-2-yl)-2,5-diphenyltetrazolium bromide) assay at concentrations of 0.5–20.0 μg/mL. The cells were incubated with the PSs followed by 24 h standing and photo-irradiated for the photoactivity test using a light-emitting diode (LED, 735–785 nm, total light dose 2 J/cm^2 for 15 min; Figure 3). Following photo-irradiation, the cells were incubated for either 12 or 24 h. Cell viability (%) was estimated based on the mitochondrial activity of reduced form of nicotinamide adenine dinucleotide (NADH) dehydrogenase (Tables S2 and S3).

Upon photo-irradiation, all compounds showed reduced cell viability consistent with increased concentration as well as incubation time. At the 12 h incubation time, GNP1 displayed high photoactivity having half-maximal inhibitory

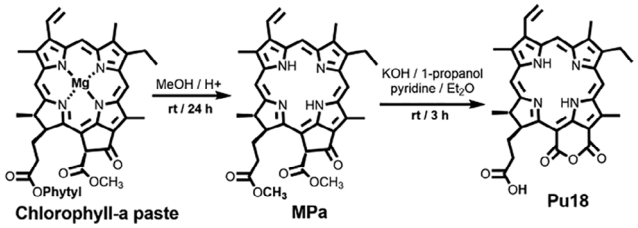

Scheme 1. Synthesis of Pu18.

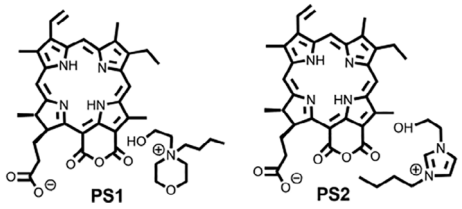

Figure 1. Structures of IL-type PSs.

concentration (IC_{50}) value of 0.38 μg/mL (Figure 3(a), Table 1), exhibiting the excellent delivery effects of the GNP as well as chemical and structural properties of morpholinium (Figure S8),[25] whereas GNP2 had very low photocytotoxicity with IC_{50} of >20.0 μg/mL. GNP1 revealed the same high photoactivity (constant IC_{50} value) at the 24 h incubation time (Figure 3(b), Table 1), indicating the fast delivery of the GNP into the tumor cells.[9] Therefore, GNP1 showed 34–37-fold higher enhanced photoactivity compared to free PS1 because of the excellent drug delivery effect of the GNP based on the EPR-effect and accumulation by endocytosis into the cells.[18–20] On the other hand, GNP2 showed good photoactivity with an IC_{50} of 4.34 μg/mL, which is 3.6-fold higher compared to that shown by free PS2. GNP1 had 11-fold higher photoactivity than GNP2 in which different result between GNP1 and GNP2 might be attributed by the faster drug delivery effect of GNP1 compared with GNP2 based on the corresponding each IL-type PS ability. Thus, the photoactivity results were significantly affected by different IL-type PS (IL-dependent).

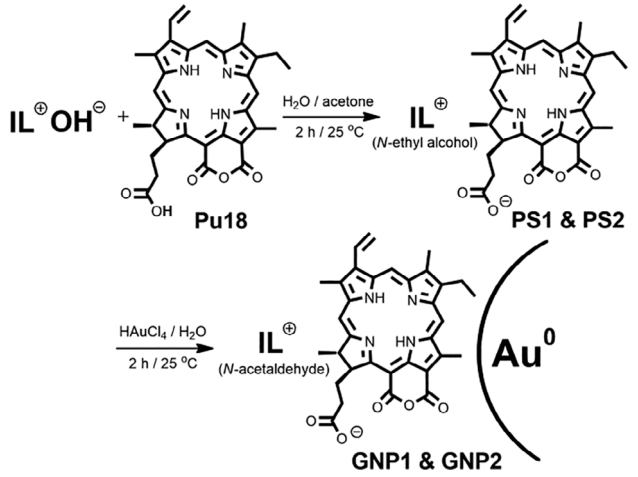

Scheme 2. Preparation of GNPs.

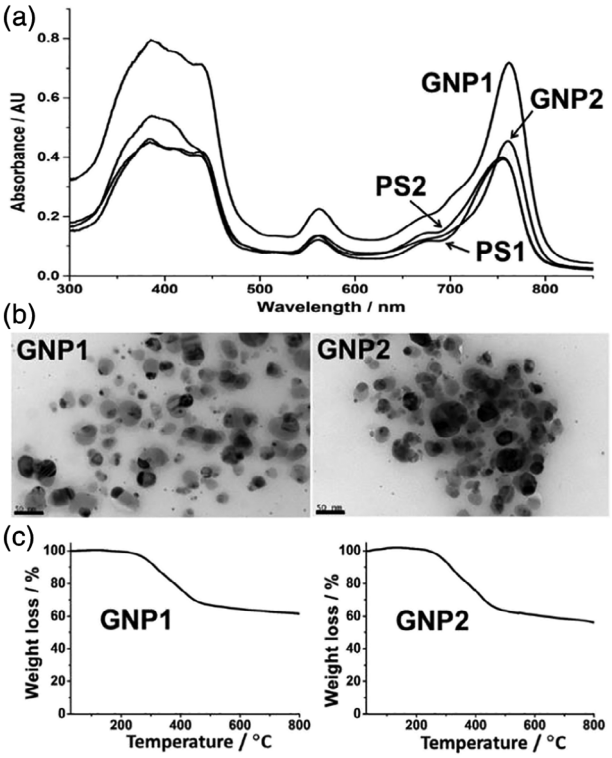

Figure 2. (a) UV–Vis spectra of PS1 (λ_{max}, 755 nm), PS2 (λ_{max}, 754 nm), GNP1 (λ_{max}, 762 nm), and GNP2 (λ_{max}, 761 nm) (10 μg/mL in water). (b) TEM images of GNP1 and GNP2. Scale bar: 50 nm. (c) TGA analysis of GNP1 (PS: Au = 37:63) and GNP2 (PS: Au = 42:58).

PS1 and GNP1 exhibited no dark toxicity, whereas PS2 and GNP2 had little dose-dependent dark toxicity.

The high cellular uptake and localization of PS1, PS2, GNP1, and GNP2 in A549 cells was confirmed by confocal laser scanning microscopy (CLSM) playing fluorescence imaging of the PS in each compound (Figure 4). CLSM images indicated that GNP1 and GNP2 have efficient ability of PS (shown in red) transport into the cells compared to PS1 and PS2 (free PS), inducing higher photoactivity (Figure 3). Most of the PSs were accumulated in cytoplasm of the cell.[9,11] Before irradiation (dark), cell morphology was similar across all compounds, however, after irradiation (light), GNP1-treated cells exhibited the presence of apoptotic bodies.[26] In addition, very few cells survived after the GNP1 treatment, indicating most that of the tumor cells were destroyed by its high photodynamic action, consistent with the very low IC_{50} value (Table 1).

In conclusion, two GNPs were synthesized using corresponding water-soluble IL-type PSs and then characterized. IL-type PSs have two important roles: (1) acting as self-reducing agents of the gold ion and (2) as a stabilizer for the GNPs. GNP1 displays higher absorption intensity and high photoactivity without dark toxicity, which was confirmed by CLSM imaging. Photocytotoxicity and dark toxicity of both PSs and their corresponding GNPs were significantly different based on the type of IL used, indicating an IL-dependent

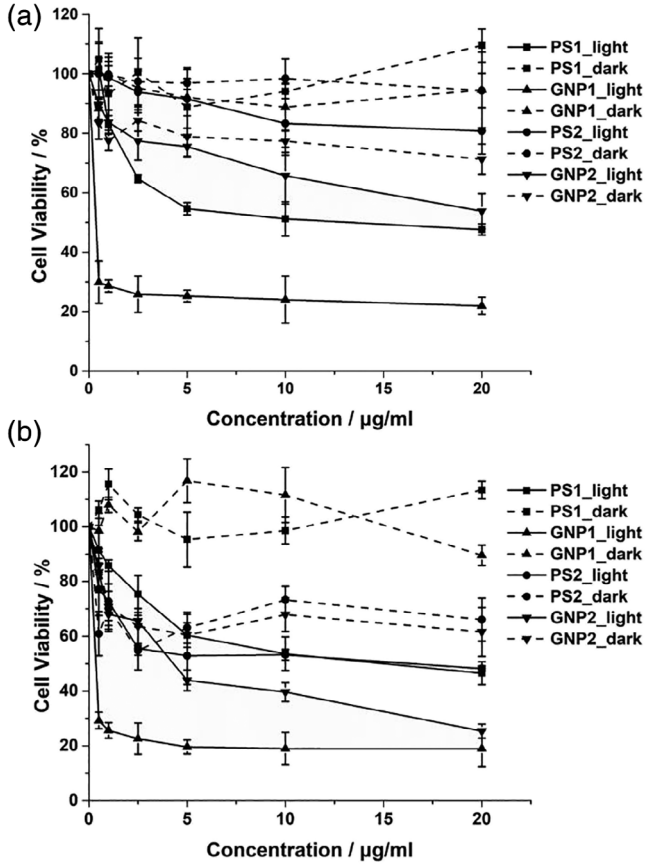

Figure 3. Cell viability against A549 cells after (a) 12 h and (b) 24 h of incubation times following PS1, PS2, GNP1, and GNP2 treatment at concentrations of 0.5–20.0 μg/mL. From MTT assay cell viability (%) was determined by before (dark) and after (light) photo-irradiation (total light dose 2 J/cm^2 for 15 min with a 735–785 nm LED). Error bars show the standard deviation of replicated three experiments.

Table 1. IC_{50} values (μg/mL) of PS1, PS2, GNP1, and GNP2 after photo-irradiation following 12 and 24 h incubation.

Compound/incubation time	PS1	PS2	GNP1	GNP2
12 h	12.92	>20.0	0.38	>20.0
24 h	14.15	15.57	0.38	4.34

phenomenon. This study could be useful not only for the design and synthesis of new IL-type PSs but for development of enhanced PDT using water-soluble IL and GNPs.

Experimental

Synthesis of IL-Type PSs. A Pu18 solution (25 mg, 0.044 mmol in acetone [5 mL]) was mixed with an each IL aqueous solution (0.044 mmol in water [10 mL]). This mixed solution was sonicated for 5 min followed by stirring for 2 h at room temperature. After evaporation, the aqueous solution was freeze-dried to obtain each PS as a black solid.

Preparation of GNPs Seed Solution. Each PS solution (0.002 M, 5 mL) was mixed with $HAuCl_4$ (0.001 M, 2.5 mL) in a 50 mL flask and stirred for 2 h at room temperature. During this reaction, the solution changed from yellow-color to greenish-black-color. The solution was stored at room temperature.

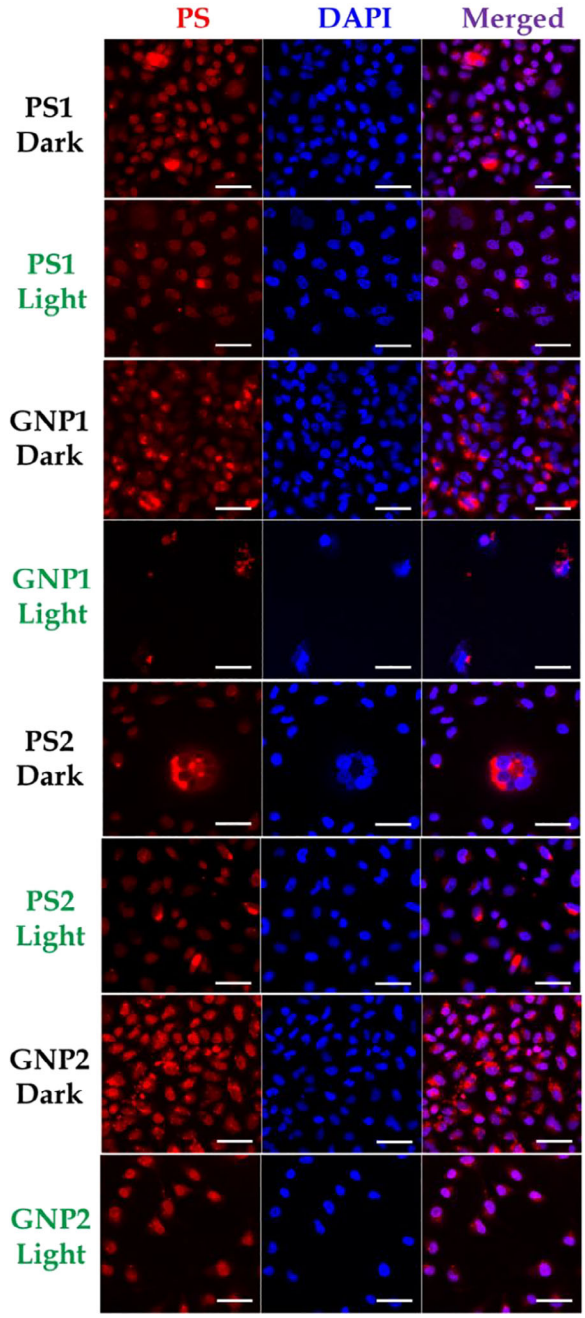

Figure 4. Images of A549 cells using CLSM before (dark) and after (light) irradiation (total light dose was 2 J/cm^2) for PS1, PS2, GNP1, and GNP2. PS (chlorins, red), DAPI nuclear dye (blue), and merged images. Scale bar: 10 μm.

Preparation of Growth Solution for GNPs. A $HAuCl_4$ solution (0.001 M, 25 mL) was added to each PS solution (0.002 M, 25 mL) in a 250-mL flask (the color changed from yellow to green). Then an $AgNO_3$ solution (0.005 M, 1 mL) was added to the mixture. The seed solution (200 μL) was added to the mixed solution and the flask was left

immobile, to allow growing of the seeds in the solution. Mostly, the solution color was gradually changed within a few minutes. After a few hours, the GNPs were produced and washed with water several times followed by a centrifugation at 10 000 rpm for 10 min for several times to remove free PSs to obtain GNPs as a greenish-black solid.

Cell Culture and Photo-Irradiation. From the cell line bank of the Seoul National University Cancer Research Center A549 (human lung carcinoma) cells were obtained. The cells were grown in a media solution contains RPMI-1640 (Sigma-Aldrich, Munich, Germany) with 10% fetal bovine serum and 1% penicillin at 37 °C in a humidified atmosphere with 5% CO_2 in air. In the procedures, phosphate-buffered saline (PBS, Sigma-Aldrich), trypsin-ethylene diamine tetraacetic acid (EDTA) solution, an incubator (37 °C, 5% CO_2), SynergyHT fluorescence multi-detection reader (BioTek, Winooski, VT, USA), and optical microscope (model CK40-32 PH; Olympus, Tokyo, Japan) were used. PDT was performed using a LED (735–785 nm, total light dose 2 J/cm^2 for 15 min).

MTT Assay and Cell Viability. Cells ($1 \times 10,^5$ 100 μL) were placed in a 96-well microplate. A 24 h later, the medium was removed and the plates were washed with PBS for two times. Mixed medium (100 μL) of each PS and GNPs were added to the each well. A 24 h later, the medium was removed and the plates washed with PBS for three times, followed by adding fresh medium (100 μL). After irradiation (2 J/cm^2, 15 min) of the plates, the MTT assay was performed to evaluate PDT activity. In each well MTT solution was added and incubated for 1 h, and measured absorbance at 450 nm using a fluorescence multi-detection reader. The plates were photo-irradiated followed by 12 and 24 h incubations. Each group consisted of three wells for three replicate experiments.

Analysis of Cell Morphology and Number. A549 cells (1×10^4 cells) were plated on confocal dishes and incubated. A 24 h later, the medium was removed and dishes were washed with PBS for three times. Then each PS and GNPs (1 μM) were added to the dishes. A 24 h later, the dishes were washed with PBS for three times. After the fixation solution was added (10 min), followed by washing with PBS and staining with diamidino-2-phenylindole (DAPI, 200 nM), cell images were acquired using CLSM by an LSM 510 META microscope (Carl Zeiss,Oberkochen, Germany).

Acknowledgments. This research was supported by the National Research Foundation (NRF) of Korea grant funded by the Korea government (NRF-2017R1A2B4010615).

Supporting Information. Additional supporting information is available in the online version of this article.

References

1. T. J. Greaves, C. J. Drummond, *Chem. Rev.* **2008**, *108*, 206.
2. P. Wasserscheid, W. Keim, *Angew. Chem. Int. Ed.* **2000**, *39*, 3772.
3. H. J. Ryu, L. Sanchez, H. A. Keul, A. Raj, M. R. Bockstaller, *Angew. Chem. Int. Ed.* **2008**, *47*, 7639.
4. T. Welton, P. Wasserscheid Eds., *Ionic Liquids in Synthesis*, 2nd ed., Wiley VCH, Weinheim, **2008**.
5. M. Moniruzzaman, K. Nakashima, N. Kamiya, M. Goto, *Biochem. Eng. J.* **2010**, *48*, 295.
6. R. Ferraz, L. C. Branco, I. M. Marrucho, J. M. M. Araújo, L. P. N. Rebelo, M. N. da Ponte, C. Prudêncio, J. P. Noronha, Ž. Petrovski, *Med. Chem. Commun.* **2012**, *3*, 494.
7. S. Y. Choi, H. Rodríguez, A. Mirjafari, D. F. Gilpin, S. McGrath, K. R. Malcolm, M. M. Tunney, R. D. Rogers, T. McNally, *Green Chem.* **2011**, *13*, 1527.
8. P. Zhang, H. Huang, S. Banerjee, G. J. Clarkson, C. Ge, C. Imberti, P. J. Sadler, *Angew. Chem. Int. Ed.* **2019**, *58*, 2350.
9. E. S. Kang, T. H. Lee, Y. Liu, K.-H. Han, W. K. Lee, I. Yoon, *Int. J. Mol. Sci.* **2019**, *20*, 4344.
10. J.-E. Chang, Y. Liu, T. H. Lee, W. K. Lee, I. Yoon, K. Kim, *Int. J. Mol. Sci.* **2018**, *19*, 1596.
11. I. Yoon, J. H. Kim, J. Z. Li, W. K. Lee, Y. K. Shim, *Inorg. Chem.* **2014**, *53*, 3.
12. J. Nam, N. Won, H. Jin, H. Chung, S. Kim, *J. Am. Chem. Soc.* **2009**, *131*, 13639.
13. Y. Cheng, A. C. Samia, J. D. Meyers, I. Panagopoulos, B. Fei, C. Burda, *J. Am. Chem. Soc.* **2008**, *130*, 10643.
14. P. Vijayaraghavan, C.-H. Liu, R. Vankayala, C.-S. Chiang, K. C. Hwang, *Adv. Mater.* **2014**, *26*, 6689.
15. O. Penon, T. Patiño, L. Barrios, C. Nogués, D. B. Amabilino, K. Wurst, L. Pérez-García, *Chemistry OPEN* **2015**, *4*, 127.
16. B. D. Chithrani, A. A. Ghazani, W. C. W. Chan, *Nano Lett.* **2006**, *6*, 662.
17. X. Ma, Y. Wu, S. Jin, Y. Tian, X. Zhang, Y. Zhao, L. Yu, X.-J. Liang, *ACS Nano* **2011**, *5*, 8629.
18. V. P. Torchilin, *Adv. Drug Deliv. Rev.* **2006**, *58*, 1532.
19. B. Lkhagvadulam, J. H. Kim, I. Yoon, Y. K. Shim, *J. Porphyrins Phthalocyanines* **2012**, *16*, 331.
20. B. Lkhagvadulam, J. H. Kim, I. Yoon, Y. K. Shim, *Biomed. Res. Int.* 2013, **2013**, 10 pages.
21. G. Zheng, W. R. Potter, S. H. Camacho, J. R. Missert, G. Wang, D. A. Bellnier, B. W. Henderson, M. A. J. Rodgers, T. J. Dougherty, R. K. Pandey, *J. Med. Chem.* **2001**, *44*, 1540.
22. D. Demberelnyamba, M. Ariunaa, Y. K. Shim, *Int. J. Mol. Sci.* **2008**, *9*, 864.
23. Y.-H. Chen, C.-Y. Tsai, P.-Y. Huang, M.-Y. Chang, P.-C. Cheng, C.-H. Chou, D.-H. Chen, C.-R. Wang, A.-L. Shiau, C.-L. Wu, *Mol. Pharm.* **2007**, *4*, 713.
24. J. D. Gibson, B. P. Khanal, E. R. Zubarev, *J. Am. Chem. Soc.* **2007**, *129*, 11653.
25. J.-H. Cha, K.-S. Kim, S. Choi, S.-H. Yeon, H. Lee, H. S. Kim, H. Kim, *Korean J. Chem. Eng.* **2005**, *22*, 945.
26. W. Jiang, B. Y. S. Kim, J. T. Rutka, W. C. W. Chan, *Nature Nanotech.* **2008**, *3*, 145.

